ELSEVIER

www.elsevier.nl/locate/jorganchem

Journal of Organometallic Chemistry 602 (2000) 59–64

Journal of Organometallic Chemistry

Rh(acac)(CO)(PR_3) and Rh(oxinate)(CO)(PR_3) complexes—substitution chemistry and structural aspects

Walter Simanko [a], Kurt Mereiter [b], Roland Schmid [a], Karl Kirchner [a,*1], Anna M. Trzeciak [c], Jozef J. Ziołkowski [c,*2]

[a] *Institute of Inorganic Chemistry, Technical University of Vienna, Getreidemarkt 9, A-1060 Vienna, Austria*
[b] *Institute of Mineralogy, Crystallography, and Structural Chemistry, Technical University of Vienna, Getreidemarkt 9, A-1060 Vienna, Austria*
[c] *Faculty of Chemistry, University of Wrocław, 14 F. Joliot-Curie str., 50-383 Wrocław, Poland*

Received 29 November 1999; received in revised form 7 February 2000; accepted 14 February 2000

Abstract

The substitution of CO in Rh(acac)($CO)_2$ by the phosphorus ligands $P(OPh)_3$, $P(NC_4H_4)_3$, and $PPh_2(NC_4H_4)$ has been studied kinetically by stopped-flow spectrophotometry as a function of temperature. With $P(OPh)_3$ and $P(NC_4H_4)_3$, both CO ligands are replaced in a stepwise fashion via the intermediate Rh(acac)(CO)(PR_3). However, the disubstituted complexes Rh(acac)($PR_3)_2$ are thermodynamically unstable. Judged from the activation parameters, the individual steps are associative processes. In the case of $PPh_2(NC_4H_4)$ only the monosubstituted complex is formed. The differences in the substitution rates as well as the stability of the various products are largely dominated by electronic (e.g. basicity) effects. X-ray structures of some of the mono-substituted complexes are given. In addition, also the reaction of Rh(oxinate)($CO)_2$ with $P(OPh)_3$ has been studied kinetically showing that oxinate has a labilizing effect relative to acetylacetonate

Keywords: Rhodium; Ligand substitution; Tertiary phosphines; Kinetics; Acetylacetonate

1. Introduction

Rh(acac)($CO)_2$ (acac = acetylacetonate) in the presence of tertiary phosphines or phosphites (PR_3) is a well established catalytic system for hydroformylation, hydrogenation, and isomerization reactions of olefins [1–5]. For the hydroformylation process, several reaction sequences take place wherein Rh(acac)($CO)_2$ is eventually converted into the catalytically active hydrido complex $HRh(CO)(PR_3)_3$. In the first reaction step, CO is replaced by PR_3 giving Rh(acac)(CO)(PR_3) [6,7]. The substitution of the second CO ligand is rather sluggish requiring the removal of free CO by purging with an inert gas. Even then, however, strong π-acceptors such as $PR_3 = P(OPh)_3$ or $P(NC_4H_4)_3$ are necessary in order to obtain di-substituted Rh(acac)($PR_3)_2$. Weak π-acceptors, even when used in large excess, afford only monosubstituted products [4,6,7].

In the present paper we report on the synthesis and structure of Rh(acac)(CO)(PR_3) and Rh(oxinate)(CO)(PR_3) (oxinate = quinolin-8-olate) complexes as well as their substitution kinetics with some tertiary phosphines and phosphites. The kinetic and thermodynamic analyses will aid in understanding the factors that govern the formation of Rh(acac)(CO)(PR_3) and Rh(acac)($PR_3)_2$ and their oxinate analogs. Note that the reaction of Rh(acac)($CO)_2$ with $P(OPh)_3$ had already been partially investigated previously by some of us [8]. Furthermore, the substitution of CO in Rh(β-diketone)($CO)_2$ complexes by 1,5-cyclooctadiene (COD) [9] and $P(OPh)_3$ [8] has been reported. Studies of COD substitution in Rh(β-diketone)(COD) by $P(OPh)_3$ have also shown that the reaction rate is strongly dependent on the electronic properties of the substituents at the β-diketone ligand [10].

[1] *Corresponding author. Tel.: +43-1-5880115341; fax: +43-1-5880115399; e-mail: kkirch@mail.zserv.tuwien.ac.at

[2] *Corresponding author. Tel.: +48-71-3204254; fax: +48-71-3282348.

0022-328X/00/$ - see front matter
PII: S0022-328X(00)00118-2

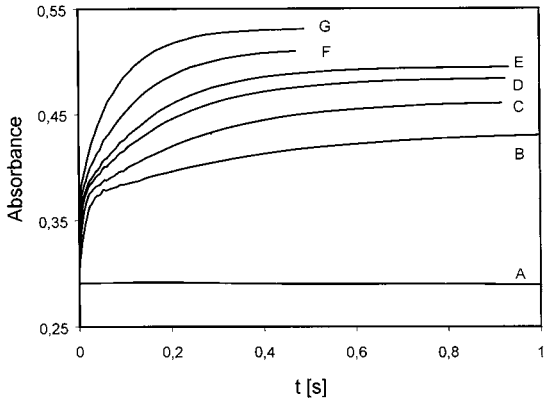

Fig. 1. Typical biphasic time profiles for the reaction of $Rh(acac)(CO)_2$ with $P(OPh)_3$ in toluene at 25°C. The concentrations are [Rh]: 0.05 mM, $[P(OPh)_3]$: 0.0 (**A**), 0.25 (**B**), 0.5 (**C**), 0.75 (**D**), 1.0 (**E**), 1.5 (**F**), and 2.5 mM (**G**).

2. Results and discussion

2.1. $Rh(acac)(CO)_2$

The reactions shown in Eqs. (1) and (2) have been studied by means of stopped flow spectrophotometry. The details of data collection and establishment of the rate law are presented in the Experimental Section. For $P(OPh)_3$ the data fit a two-term rate law involving irreversible formation

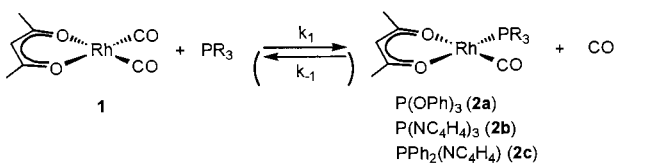

(1)

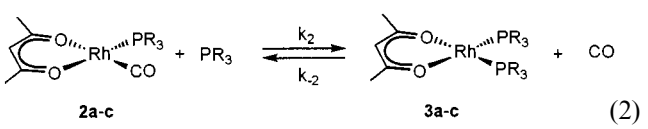

(2)

of the intermediate $Rh(acac)(CO)(P(OPh)_3)$ (**2a**) followed by reversible formation of $Rh(acac)(P(OPh)_3)_2$ (**3a**). Typical time profiles as a function of the concentration of $P(OPh)_3$ are depicted in Fig. 1. Thus, the second reaction does not go to completion under the selected experimental conditions. The kinetic results are summarized in Table 1. The individual steps (k_1, k_2, k_{-2}) are characterized by large and negative entropies of activation and are thus associative in nature. It is further seen that the barrier of CO substitution is somewhat higher in **2a** compared to **1**. This is interpreted in terms of the higher σ-donor strength of the phosphite ligand compared to CO, thereby strengthening the remaining Rh–CO bond via an increased back-donation. In this case the higher barrier is predominantly electronic in origin. The small equilibrium constant $K_{2,-2}$ obtained from combining the rate constants k_2 and k_{-2} shows that the equilibrium is shifted towards the monosubstituted complex **2a** even at high phosphite concentrations. Due to the reversibility of the second step, the overall reaction rate becomes a function of the total Rh complex concentration as a result of its effect on the CO concentration as mentioned elsewhere [8]. The k_{-2} path has also been studied by treatment of **3a** with CO dissolved in toluene. These CO solutions have been prepared from a stock solution of CO in toluene (solubility of CO at 25°C is ca. 6.87 mmol l^{-1}). The second order rate constant of 2.2×10^4 M^{-1} s^{-1} obtained from the concentration time curves is in good agreement with k_{-2} in Table 1, considering the rather little dependability of the CO concentrations.

As has been established by ^1H- and $^{31}P\{^1H\}$-NMR studies [4], $P(NC_4H_4)_3$ reacts analogously to $P(OPh)_3$ replacing consecutively both CO ligands. Note the slowing down of the k_1 step by a factor of about 55 compared to $P(OPh)_3$. Unfortunately, the second reaction step could not be measured by photometric methods since **2b** and **3b** are too similar with respect to their absorption spectra in the UV–vis range.

Finally, with $PPh_2(NC_4H_4)$ as the reagent, the overall reaction becomes very unfavorable. The second step is

Table 1
Kinetic and equilibrium data[a] for the conversion of **1** to **3** in toluene at 25°C

PR_3	Step	$\Delta H^{\ddagger}$ or $\Delta H°$ (kcal mol^{-1})	$\Delta S^{\ddagger}$ or $\Delta S°$ (cal K^{-1} mol^{-1})	k (M^{-1} s^{-1}) or K
$P(OPh)_3$	k_1	2 ± 1	-27 ± 2	2.6×10^5
	k_2	6 ± 2	-22 ± 6	4.5×10^3
	k_{-2}	6 ± 3	-19 ± 10	2.8×10^4
	$K_{2,-2}$	0.2	-3.1	0.2
$P(NC_4H_4)_3$	k_1[b]	2 ± 1	-30 ± 2	4.7×10^4
$P(NC_4H_4)Ph_2$	k_1[c]			2.4×10^3
	k_{-1}[c]			3.6×10^4
	$K_{1,-1}$[c]			6.7×10^{-2}

[a] The large error limits are due to the small absorbance changes during the reactions.
[b] The k_2,k_{-2} path was not observable because of insufficient absorbance changes.
[c] Insufficient absorbance change at higher temperatures.

Table 2
Selected properties of the Rh(acac)(CO)(PR_3) and Rh(oxinate)(CO)($P(OPh)_3$) complexes

PR_3	ν_{CO} [a,b] (cm^{-1})	^{31}P [a] (ppm)	^1J(Rh–P) [a] (Hz)	Cone angle [c] (°)	Rh–P (Å)	Rh–O (Å) (*trans* to P)	k_1 (25°C) (M^{-1} s^{-1})	ΔH_{rxn} [c] (kcal mol^{-1})
$P(NC_4H_4)_3$	2012	102.5	251	141	2.166(1)	2.054(2)	4.7×10^4	3.6
$P(OPh)_3$	2006	212.1	293	136	2.170(1)	2.063(2)	2.6×10^5	4.2
$P(NC_4H_4)_2Ph$	2002	104.7	218	150				3.8
$P(NC_4H_4)Ph_2$	1990	90.0	194	154	2.223(1)	2.078(2)	2.4×10^3	4.1
PPh_3 [d]	1975	48.6	180	145	2.243(2)	2.087(4)		4.8
$P(OPh)_3$ [e]	1983	126.3	281	136	2.186(1)		$>3\times10^5$	

[a] Ref. [4].
[b] Ref. [20]
[c] Ref. [21]
[d] Ref. [22]
[e] Rh(oxinate)(CO)($P(OPh)_3$)

not observed at all, and the first one is largely shifted to the educts. The much smaller rate constant k_1 is plausible since $PPh_2(NC_4H_4)$ is a weaker π-acceptor and, concomitantly, a stronger σ-donor. No temperature dependence study has been undertaken in view of the small absorbance changes in the UV–vis region. This situation could not be remedied by the insertion of CF_3 or phenyl groups in the acac moiety. Qualitatively, as judged from NMR spectroscopy, the reaction rates of the first substitution step were similar to that of the parent complex

The differences in the rate of CO substitution by the series of phosphorus ligands as well as in the thermodynamic stability of the products is remarkable. As noted above, this result appears to be largely an electronic, i.e. basicity, effect. Possible steric components remain masked in view of the similar sizes, expressible by their cone angles, of the ligands used (Table 2). It should be noted that the rate constants k_1 correlate neither with ΔH_{rxn} nor ν_{CO} but to some extent with the $^{31}P\{^1H\}$-NMR shifts and the $^1J_{(Rh-P)}$ coupling constants. However, there is no a priori reason for an intrinsic relationship between NMR chemical shifts or coupling constants and chemical reactivity (Direct relationships between chemical shifts and rate constants have been described elsewhere [11,12]). On the other hand, there is a correlation between the ν_{CO} values and the Rh–P and Rh–O (*trans* to P) distances of complexes **2** (Table 2). The latter have been taken from the X-ray structures of **2a** and **2c** depicted in Figs. 2 and 3 with selected bond distances and angles reported in the captions. Summing up, the PR_3 ligands can be arranged in the following order of decreasing π and increasing σ-donor properties (and *trans* influence of the ligands): $P(NC_4H_4)_3 > P(OPh)_3 > PPh_2(NC_4H_4) > PPh_3$. Based on our kinetic studies, qualitatively CO substitution is faster in the case of strong π-acceptor ligands forming stronger Rh–P bonds, while an increased σ-donor strength of the entering ligand causes the rate to decrease. At present, however, we cannot explain the fact that

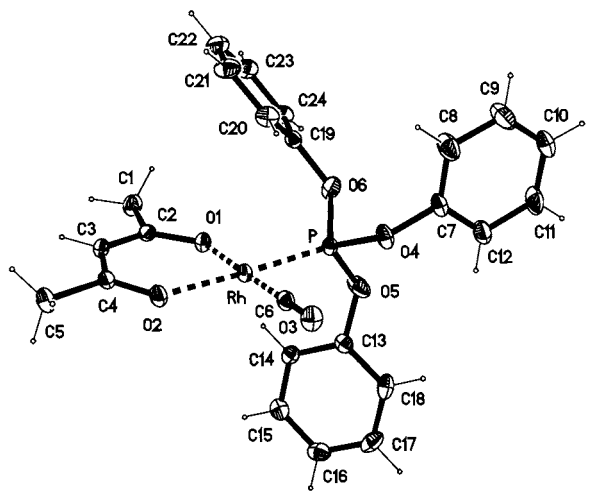

Fig. 2. Structural view of Rh(acac)(CO)($P(OPh)_3$) (**2a**) showing 20% thermal ellipsoids. Selected bond lengths (Å) and angles (°): Rh–C(6) 1.823(3), Rh–O(1) 2.040(2), Rh–O(2) 2.063(2), Rh–P 2.170(1), C(6)–Rh–O(1) 178.55(9), O(2)–Rh–P 177.54(5).

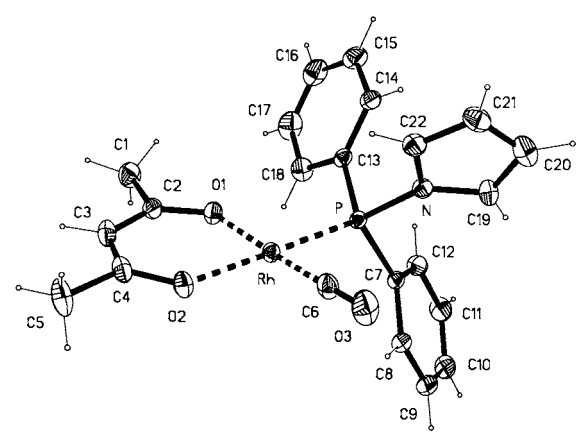

Fig. 3. Structural view of Rh(acac)(CO)($PPh_2(NC_4H_4)$) (**2c**) showing 20% thermal ellipsoids. Selected bond lengths (Å) and angles (°): Rh–C(6) 1.817(2), Rh–O(1) 2.033(2). Rh–O(2) 2.078(2), Rh–P 2.223(1), C(6)–Rh–O(1) 177.26(9), O(2)–Rh–P 179.58(4).

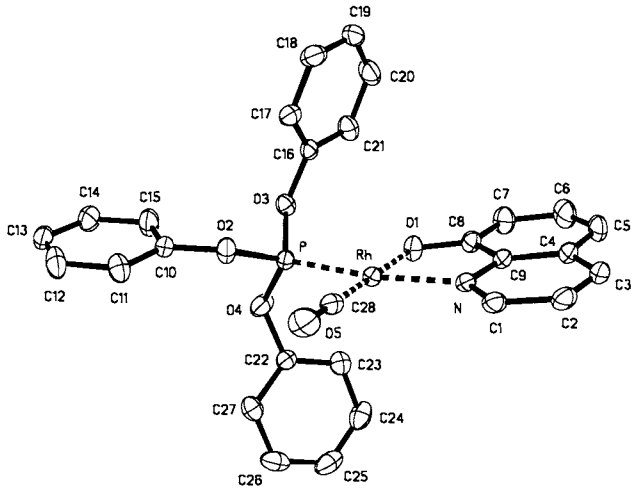

Fig. 4. Structural view of Rh(oxinate)(CO)($P(OPh)_3$) (**5**) showing 20% thermal ellipsoids. Selected bond lengths (Å) and angles (°): Rh–C(28) 1.813(3), Rh–O(1) 2.022(2). Rh–N 2.097(2), Rh–P 2.186(1), O(1)–C(8) 1.326(3), C(28)–O(5) 1.146(3), C(28)–Rh–O(1) 179.6(1), N–Rh–P 169.9(1), Rh–O(1)–C(8) 113.3(1), Rh–N–C(1) 130.8(1), Rh–N–C(9) 110.4(1).

Table 3
Kinetic and equilibrium data for the conversion of **4** to **6** in acetone at 25°C

Step	$\Delta H^{\ddagger}$ or $\Delta H°$ (kcal mol^{-1})	$\Delta S^{\ddagger}$ or $\Delta S°$ (cal K^{-1} mol^{-1})	k (M^{-1} s^{-1}) or K
k_1 [a]			$>3\times10^5$
k_2	1.8 ± 0.2	-38 ± 6	1.6×10^3
k_{-2}	4.4 ± 0.7	-22 ± 4	5.0×10^4
$K_{2,-2}$	-2.6	-16	0.03

[a] Too fast to measure by the stopped-flow method.

$P(OPh)_3$ reacts faster than $P(NC_4H_4)_3$ and apparently more subtle differences between these ligands have to be taken into account.

2.2. Rh(oxinate)$(CO)_2$

For comparison with the acac system, we have also studied the CO substitution in Rh(oxinate)$(CO)_2$ (**4**) by $P(OPh)_3$. Complex **4** reacts with $P(OPh)_3$ to give the Rh(oxinate)(CO)($P(OPh)_3$) (**5**). Of the two possible isomers only the one with $P(OPh)_3$ *trans* to the nitrogen atom of the oxinate ligand is formed. Noteworthy, the same isomer has been found for the analogous complex Rh(oxinate)(CO)(PPh_3). This may be explained by the stronger *trans* influence of nitrogen. The ν_{CO} band in the IR spectrum of **5** was found at 1983 cm^{-1} and is shifted to higher frequencies by about 20 cm^{-1} compared to Rh(β-diketone)(CO)($P(OPh)_3$). This may be attributed to the stronger donor properties of the oxinate ligand. The $^{31}P\{^1H\}$-NMR data, however, remain unchanged. Both the chemical shift and the $^1J_{(Rh-P)}$ coupling constant are similar to those in analogous β-diketone complexes.

In order to ascertain the ligand disposition in **5** the compound has been recrystallized from MeOH and subjected to an X-ray structure determination. A view of the molecular structure is given in Fig. 4 with important bond lengths and angles given in the caption. Thus, rhodium adopts a slightly distorted square planar coordination with a r.m.s. deviation from planarity of 0.030 Å and with the phosphite ligand *trans* to oxinate-N. The same feature has been encountered in a number of related compounds and the PPh_3 analogue of Rh(oxinate)(CO)(PPh_3), for which bond lengths of Rh–N = 2.098, Rh–O = 2.041, Rh–C = 1.785, and Rh–P = 2.261 Å were reported [13]. The very significant difference in the Rh–P bond length relative to that of the phosphite complex **5** (Rh–P = 2.186 Å) is a consequence of $P(OPh)_3$ being the weaker σ-donor but a much better π-acceptor than PPh_3, resulting in a relatively strong Rh–P bond. Similar observations have been made for a pair of carbonyl-(2-quinolinecarboxylato-*N*,*O*)-triphenylphosphine/triphenylphosphite Rh(I) complexes [14].

The reactions shown in Eqs. (3) and (4) have been studied by means of stopped flow spectrophotometry. In contrast to Rh(acac)$(CO)_2$, the substitution of the first CO ligand by $P(OPh)_3$ was too fast to measure with our stopped-flow equipment.

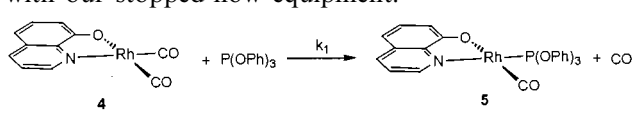

(3)

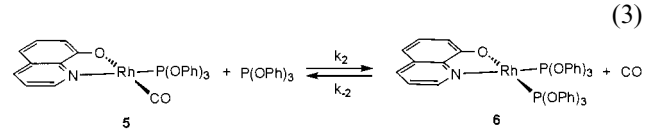

(4)

Thus only a lower limiting value equal to about 3×10^5 M^{-1} s^{-1} can be given. In line with the Rh(acac) system, the second substitution step is reversible. The kinetic results are summarized in Table 3. Again, the formation of the bisphosphite rhodium complex **6** is unfavorable. The Rh(oxinate)($P(OPh)_3$))$_2$ complex was isolated from the CO-free solution.

3. Experimental

3.1. General methods

All reactions were performed under an inert atmosphere of purified argon by using Schlenk techniques and/or a glove box. All chemicals were standard reagent grade and used without further purification. The solvents were purified and dried according to standard procedures and stored over 4 Å molecular sieves.

The deuterated solvents were purchased from Aldrich and dried over 4 Å molecular sieves. $Rh(acac)(CO)_2$ (**1**) [15], $Rh(acac)(CO)(P(OPh)_3)$ (**2a**) [7], $Rh(acac)(P(OPh)_3)_2$ (**3a**) [16], $Rh(acac)(CO)(P(NC_4H_4)_3)$ (**2b**) [4], $Rh(acac)(P(NC_4H_4)_3)_2$ (**3b**) [4], $[Rh(acac)(CO)(PPh_2(NC_4H_4))$ (**2c**) [4] and $Rh(oxinate)(CO)_2$ (**4**) [15] were prepared according to the literature. Pyrrolylphosphines were obtained as described elsewhere [17]. ^1H-, $^{13}C\{^1H\}$-, and $^{31}P\{^1H\}$-NMR spectra were recorded on a Bruker AC-250 spectrometer operating at 250.13, 62.86, and 101.26 MHz, respectively, and were referenced to $SiMe_4$ and H_3PO_4 (85%).

3.1.1. Synthesis of Rh(oxinate)(CO)(P(OPh)$_3$) (5)

To a solution of $Rh(oxinate)(CO)_2$ (0.05 g, 0.165 mmol) in methanol (0.3 ml) $P(OPh)_3$ (0.05 g, 0.164 mmol) was added. The liberated CO was removed by purging the solution with dinitrogen for 5 min. Upon slow evaporation of the solvent at about 0°C, orange crystals were formed in 85% yield. $C_{28}H_{21}NO_5PRh$ requires C, 57.45; H, 3.62; N, 2.39. Found: C, 57.2; H, 3.4; N, 2.8%. NMR (acetone-d_6, 20°C): δ_P 126.3 (d, $^1J_{Rh-P} = 281.1$ Hz). ν_{max}/cm^{-1} 1983 (CO).

3.1.2. Synthesis of Rh(oxinate)(P(OPh)$_3$)$_2$ (6)

To a solution of $Rh(oxinate)(CO)_2$ (0.05 g, 0.165 mmol) in benzene (0.3 ml) $P(OPh)_3$ (0.12 g, 0.387 mmol) was added and the solution was purged with dinitrogen for 5 min. The solvent was then removed under vaccum and the residue was washed with *n*-hexane and ethanol and dried in vacuo. Yield: 75%. $C_{45}H_{36}NO_7P_2Rh$ requires C, 62.30; H, 4.18; N, 1.61. Found: C, 62.0; H, 3.92; N, 1.83%. NMR (acetone-d_6, 20°C): δ_P 127.4 (dd, $^1J_{Rh-P} = 280.0$ Hz, $J_{PP} = 101$ Hz, P *trans* to N), 125.3 (dd, $^1J_{Rh-P} = 293.0$ Hz, $J_{PP} = 101$ Hz, P *trans* to O).

3.2. Kinetics

The stopped-flow kinetic data were obtained with a Hi-Tech SF-61 instrument. The optical signal at 320 was monitored for the reactions of $Rh(acac)(CO)_2$ and/or $Rh(acac)(CO)(PR_3)$ with PR_3. For the reaction of $Rh(oxinate)(CO)_2$ with $P(OPh)_3$ the optical signal at 340 nm was monitored. The data were collected as sets of 512 points. They all involved pseudo-first order conditions with the phosphines and phosphites (PR_3) in large excess over the rhodium complexes. The calculation of rate constants was based on a numerical integration of the family of simultaneous differential equations from Eqs. 1 and 2 (3 and 4) and nonlinear least squares regression to the experimental curves (see Fig. 1) which was carried out with the Scientist data analysis package.

3.3. X-ray structure determination

X-ray data were collected on a Siemens Smart CCD area detector diffractometer ($Mo-K_\alpha$, $\lambda = 0.71073$ Å, absorption corrections by multi-scan method). All structures were solved by direct methods using the program SHELXS-97 [18]. Structure refinement on F^2 with program SHELXL-97 [19] $Rh(acac)(CO)(P(OPh)_3)$ **2a**. $-C_{24}H_{22}O_6PRh$, M = 540.30, orthorhombic, space group *Pbcn* (No 60), $a = 18.120(5)$, $b = 9.709(3)$, $c = 26.173(8)$ Å, $V = 4605(2)$ Å^3, $T = 223(2)$ K, $Z = 8$, $\mu = 0.849$ mm^{-1}, 48834 reflections ($\theta \leq 27°$), 4991 unique reflections ($R_{int} = 0.039$) which were used in all calculations. The final $wR(F^2)$ was 0.064, $R_1 = 0.043$. $Rh(acac)(CO)(PPh_2(NC_4H_4)$ (**2c**). $-C_{22}H_{21}NO_3PRh$, $M = 481.28$, triclinic, space group $P\bar{1}$ (No 2), $a = 8.777(3)$, $b = 10.424(4)$, $c = 12.904(5)$ Å, $\alpha = 73.25(2)$, $\beta = 70.63(2)$, $\gamma = 82.74(2)°$, $V = 1065.9(7)$ Å^3, $T = 295(2)$ K, $Z = 2$, $\mu = 0.897$ mm^{-1}, 15 200 reflections ($\theta \leq 30°$), 6016 unique reflections ($R_{int} = 0.019$) which were used in all calculations. The final $wR(F^2)$ was 0.065, $R_1 = 0.032$. $Rh(oxinate)(CO)(P(OPh)_3)$ **5**. $-C_{28}H_{21}NO_5PRh$, $M = 585.34$, monoclinic, space group $P2_1/n$ (No 14), $a = 14.271(4)$, $b = 10.966(3)$, $c = 16.936(5)$ Å, $\beta = 99.24(2)°$, $V = 2530.1(12)$ Å^3, $T = 295(2)$ K, $Z = 4$, $\mu = 0.777$ mm^{-1}, 35 628 reflections ($\theta \leq 30°$), 7267 unique reflections ($R_{int} = 0.026$) which were used in all calculations. The final $wR(F^2)$ was 0.075, $R_1 = 0.045$.

4. Supplementary material

Listings of atomic coordinates, anisotropic temperature factors, complete bond lengths and angles, and least-squares planes of complexes **2a**, **2c**, and **5** can be obtained from the authors on request.

Acknowledgements

Financial support by the 'Österreichischer Akademischer Austauschdienst' is gratefully acknowledged (Project 6/99). The authors also thank Marcin Drag, MSc, for the preparation of samples for the kinetic measurements and Drs Ryszard Grzybek and Grzegorz Małecki for the synthesis of pyrrolylphosphines.

References

[1] B. Moasser, W.L. Gladfelter, D.C. Roe, Organometallics 14 (1995) 3832.
[2] A. van Rooy, E.N. Orji, P.G.J. Kramer, P.W.N.M. van Leeuwen, Organometallics 14 (1995) 34.
[3] H. Yamashita, B.L. Roan, T. Sakakura, M. Tanaka, J. Mol. Catal. 81 (1993) 255.

[4] A.M. Trzeciak, T. Głowiak, R. Grzybek, J.J. Ziołkowski, J. Chem. Soc. Dalton Trans. (1997) 1831.
[5] A.M. Trzeciak, E. Wolszczak, J.J. Ziołkowski, New J. Chem. 20 (1996) 365.
[6] F. Bonati, G. Wilkinson, J. Chem. Soc. (1964) 3156.
[7] A.M. Trzeciak, J.J. Ziołkowski, Inorg. Chim. Acta 96 (1985) 15.
[8] R. van Eldik, S. Aygen, H. Kelm, A.M. Trzeciak, J.J. Ziołkowski, Trans. Met. Chem. 10 (1985) 167.
[9] J.G. Leipoldt, S.S. Basson, J.J.J. Schlebusch, E.C. Grobler, Inorg. Chim. Acta 62 (1982) 113.
[10] J.G. Leipoldt, G.J. Lamprecht, E.C. Steynberg, J. Organomet. Chem. 397 (1990) 239.
[11] W. Leitner, M. Bühl, R. Fornika, C. Six, W. Baumann, E. Dinjus, M. Kessler, C. Krüger, A. Rufinska, Organometallics 18 (1999) 1196.
[12] G.J.J. Seyn, A. Roodt, I. Poletaeva, Y.S. Varshavsky, J. Organomet. Chem. 536 (1997) 197.
[13] J.G. Leipoldt, S.S. Basson, C.R. Dennis, Inorg. Chim. Acta 50 (1981) 121.
[14] (a) D.E. Graham, G.J. Lamprecht, I.M. Potgieter, A. Roodt, J.G. Leipoldt, Trans. Met. Chem. 16 (1991)193. (b) G.J. Lamprecht, J.G. Leipoldt, A. Roodt, Acta Crystallogr. Sect. C 47 (1991) 2209.
[15] Yu.S. Varshavsky, T.G. Tcherkasova, Zh. Neorg. Khim. 12 (1967) 1709.
[16] A.M. Trzeciak, J.J. Ziołkowski, Inorg. Chim. Acta Lett. 64 (1982) L267.
[17] K.G. Moloy, J.L. Petersen, J. Am. Chem. Soc. 117 (1995) 7696.
[18] G.M. Sheldrick, SHELXS97: Program for the Solution of Crystal Structures, University of Göttingen, Germany, 1997.
[19] G.M. Sheldrick, SHELXL97: Program for Crystal Structure Refinement, University of Göttingen, Germany, 1997.
[20] S. Serron, J. Huang and S.P. Nolan, Organometallics 17 (1998) 534.
[21] C.A. Tolman, Chem. Rev. (1977) 313.
[22] A.M. Trzeciak, J.J. Ziołkowski, J. Organomet. Chem. 429 (1992) 239.